BIOCHEMISTRY
including biophysical chemistry & molecular biology

Article

pubs.acs.org/biochemistry

Characterization of Interactions between Heparin/Glycosaminoglycan and Adeno-Associated Virus

Fuming Zhang,[†] Javier Aguilera,[‡] Julie M. Beaudet,[‡] Qing Xie,[∥] Thomas F. Lerch,[∥] Omar Davulcu,[∥] Wilfredo Colón,[‡] Michael S. Chapman,*[,∥] and Robert J. Linhardt*[,†,‡,§]

[†]Department of Chemical and Biological Engineering and [‡]Department of Chemistry and Chemical Biology, Center for Biotechnology and Interdisciplinary Studies, Rensselaer Polytechnic Institute, Troy, New York 12180, United States

[§]Departments of Biology and Biomedical Engineering, Center for Biotechnology and Interdisciplinary Studies, Rensselaer Polytechnic Institute, Troy, New York 12180, United States

[∥]Department of Biochemistry and Molecular Biology, School of Medicine, Oregon Health & Science University, Portland, Oregon 97239, United States

ABSTRACT: Adeno-associated virus (AAV) is a key candidate in the development of gene therapy. In this work, we used surface plasmon resonance spectroscopy to study the interaction between AAV and heparin and other glycosaminoglycans (GAGs). Surface plasmon resonance results revealed that heparin binds to AAV with an extremely high affinity. Solution competition studies showed that binding of AAV to heparin is chain length-dependent. AAV prefers to bind full chain heparin. All sulfo groups (especially *N*-sulfo and 6-*O*-sulfo groups) on heparin are important for the AAV−heparin interaction. Higher levels of sulfo group substitution in GAGs enhance their binding affinities. Atomic force microscopy was also performed to image AAV-2 in a complex with heparin.

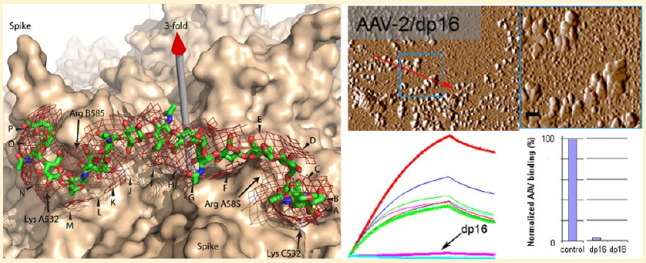

Adeno-asssociated virus (AAV) is a small DNA-containing human parvovirus that is a leading candidate vector for *in vivo* human gene therapy.[1] Gene therapy involves the delivery of genes into cells for the treatment or prevention of a disease, supplying a replacement for a faulty or missing gene, or sensitizing cells to (cancer) prodrugs.[2] The development of gene therapy currently centers mostly on basic science, but early clinical successes include demonstrated long-term efficacy in experimental treatments for retinopathies[3,4] and hemophilia B.[5] Viruses are the usual choice for gene delivery as they have naturally evolved for this purpose. The examples mentioned above show that among several viruses that have been engineered for gene therapy, AAV is increasingly prominent, considered a relatively safe vector for moderately sized genes of <5 kb. AAV is much less immunogenic than adenoviruses (no relation), and less oncogenic than retroviruses, because they transduce cells episomally or integrate with partial site specificity.[1,6−9] A lack of understanding of the tropism and cell specificity of AAV has impeded its application in gene therapy.

In vivo, multiple factors determine AAV tissue tropism, including its traversal of the endothelium, immune neutralization, and blood clearance.[10−13] Interactions with host cell molecules, starting with the primary receptor, are important both *in vivo* and *in vitro*. Cell entry for AAV starts with attachment to extracellular glycoconjugates followed by binding to one or more membrane-anchored coreceptors (or secondary receptors) prior to endosomal entry.[14−20] Virus−glycan interactions, involving glycoproteins, glycolipids, or proteoglycans (PGs), figure prominently in the cell entry of many viruses.[21] However, the importance of these virus−glycan interactions varies, particularly with respect to their role in conferring cell and tissue specificity.[22−26] Multiple lines of evidence implicate an important role of glycans in AAV attachment, including the effect of mutations at the glycan binding site on both *in vitro* cell specificity and *in vivo* tissue tropism.[11,27−32] AAV serotypes have different preferences for glycans in their attachment. AAV-2 and AAV-3 are thought to use heparan sulfate (HS) PGs as the primary receptor in cell attachment.[33,34] These serotypes, as well as AAV-6 to lesser extent, bind to heparin, a commonly used HSPG analogue.[35,36] *In vivo*, AAV-6 has a preference for glycans terminated with sialic acid, as do AAV-1, -4, and -5,[37,38] whereas AAV-9 binds to a galactose-terminated glycan.[39,40]

Heparin/HS belongs to the glycosaminoglycan (GAG) family of anionic, and often highly sulfated, complex polydisperse linear polysaccharides. An increasing number of GAG-binding proteins have been reported in the literature.[41] A number of diverse pathophysiological processes are mediated through the interaction between heparin/HS and proteins, including blood coagulation, cell growth and differentiation, host defense and viral infection, lipid transport and metabolism,

Received: July 2, 2013
Revised: August 8, 2013
Published: August 19, 2013

dx.doi.org/10.1021/bi4008676 | *Biochemistry* 2013, 52, 6275−6285

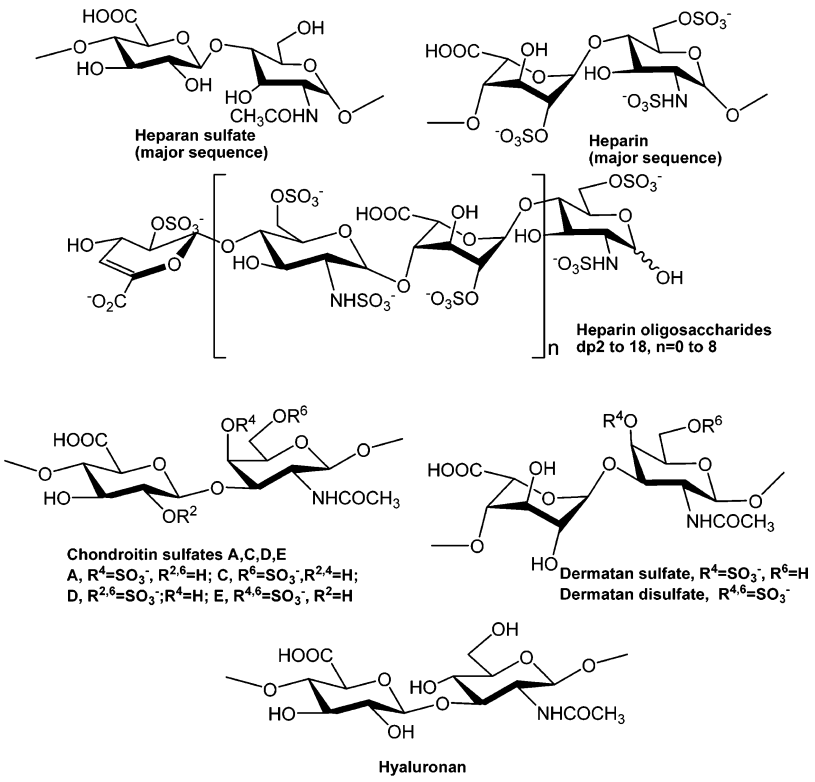

Figure 1. Chemical structures of heparin, heparin-derived oligosaccharides, and GAGs.

cell-to-cell and cell-to-matrix signaling, inflammation, and cancer.[41−44] Generally, an understanding of heparin/HS−virus particle interactions at the molecular level is of fundamental importance to biology and will aid in the development of highly specific glycan-based therapeutic agents.[41,45] For AAV, it is hoped that an improved understanding of GAG interactions will eventually allow more exquisite and rational modulation of cell attachment, transduction, and tissue tropism, beyond the gross changes demonstrated with chimeric transducing vectors.[30,35,36]

Heparin has been used as a model GAG in the study of HS−protein interaction, because it mimics the interactions of proteins with the HS present on cell surfaces and in the extracellular matrix.[21] The goal of this study is to analyze molecular interactions of heparin/GAGs with adeno-associated virus (AAV). Three different variants were used: natural human serotypes AAV-2 and AAV-6 and a chimeric gene-shuffled recombinant, AAV-DJ, which has been developed as a hepatotropic gene therapy vector. A BIAcore 3000 system was used to measure the strength of AAV−GAG interactions by surface plasmon resonance (SPR). Atomic force microscopy was also performed to image the complexes from AAV-2−heparin interaction.

EXPERIMENTAL PROCEDURES

Materials. The GAGs used were porcine intestinal heparin (16 kDa), low-molecular weight (LMW) heparin (4.8 kDa), and porcine intestinal heparan sulfate (12 kDa) (Celsus Laboratories, Cincinnati, OH), chondroitin sulfate A (20 kDa) from porcine rib cartilage (Sigma, St. Louis, MO), dermatan sulfate (also known as chondroitin sulfate B, 30 kDa, from porcine intestine, Sigma), dermatan disulfate (4,6-disulfo DS, 33 kDa, Celsus) prepared through the regioselective chemical 6-O-sulfonation of dermatan sulfate,[46] chondroitin sulfate C (20 kDa, from shark cartilage, Sigma), chondroitin sulfate D (20 kDa, from whale cartilage, Seikagaku, Tokyo, Japan), chondroitin sulfate E (20 kDa from squid cartilage, Seikagaku), and hyaluronic acid sodium salt (100 kDa, from *Streptococus zooepidemicus*, Sigma). Fully desulfated heparin (14 kDa), N-desulfated heparin (14 kDa), and 2-O-desulfated IdoA heparin (13 kDa) were all prepared using the method of Yates et al.[47] 6-O-Desulfated heparin (13 kDa) was a generous gift from L. Wang (Complex Carbohydrate Research Center, University of Georgia, Athens, GA). Heparin oligosaccharides included disaccharide [degree of polymerization of 2 (dp2)], tetrasaccharide (dp4), hexasaccharide (dp6), octasaccharide (dp8), decasaccharide (dp10), tetradecasaccharide (dp14), hexadecasaccharide (dp16), and octadecasaccharide (dp18) and were prepared from the controlled partial heparin lyase 1 treatment of bovine lung heparin (Sigma) followed by size fractionation. Chemical structures of these GAGs and heparin oligosaccharides are shown in Figure 1. Sucrose octasulfate (SOS) was from Toronto Biochemicals (Toronto, ON). Sensor SA chips were from GE Healthcare (Uppsala, Sweden). SPR measurements were performed on a BIAcore 3000 system operated using BIAcore 3000 control and BIAevaluation software (version 4.0.1).

Atomic force microscopy (AFM) was conducted on an MFP-3D atomic force microscope (Asylum Research, Santa Barbara CA) using Asylum Research version 6.22. AFM scans were performed with 2 nm (±1 nm) Super Sharp Silicon-NCLR (Non-Contact Long-cantilever Reflex-Coating) AFM cantilevers (Nano and More, Soquel, CA) on highest-grade (V1) mica sheets (Ted Pella, Redding, CA). Milli-Q water was degassed and refiltered using 0.22 μm cellulose acetate membranes (Millipore, Billerica, MA).

AAV Expression and Purification. The production of AAV-2 and AAV-DJ virus-like particles (VLPs) in SF9 cells

dx.doi.org/10.1021/bi4008676 | *Biochemistry* 2013, 52, 6275−6285

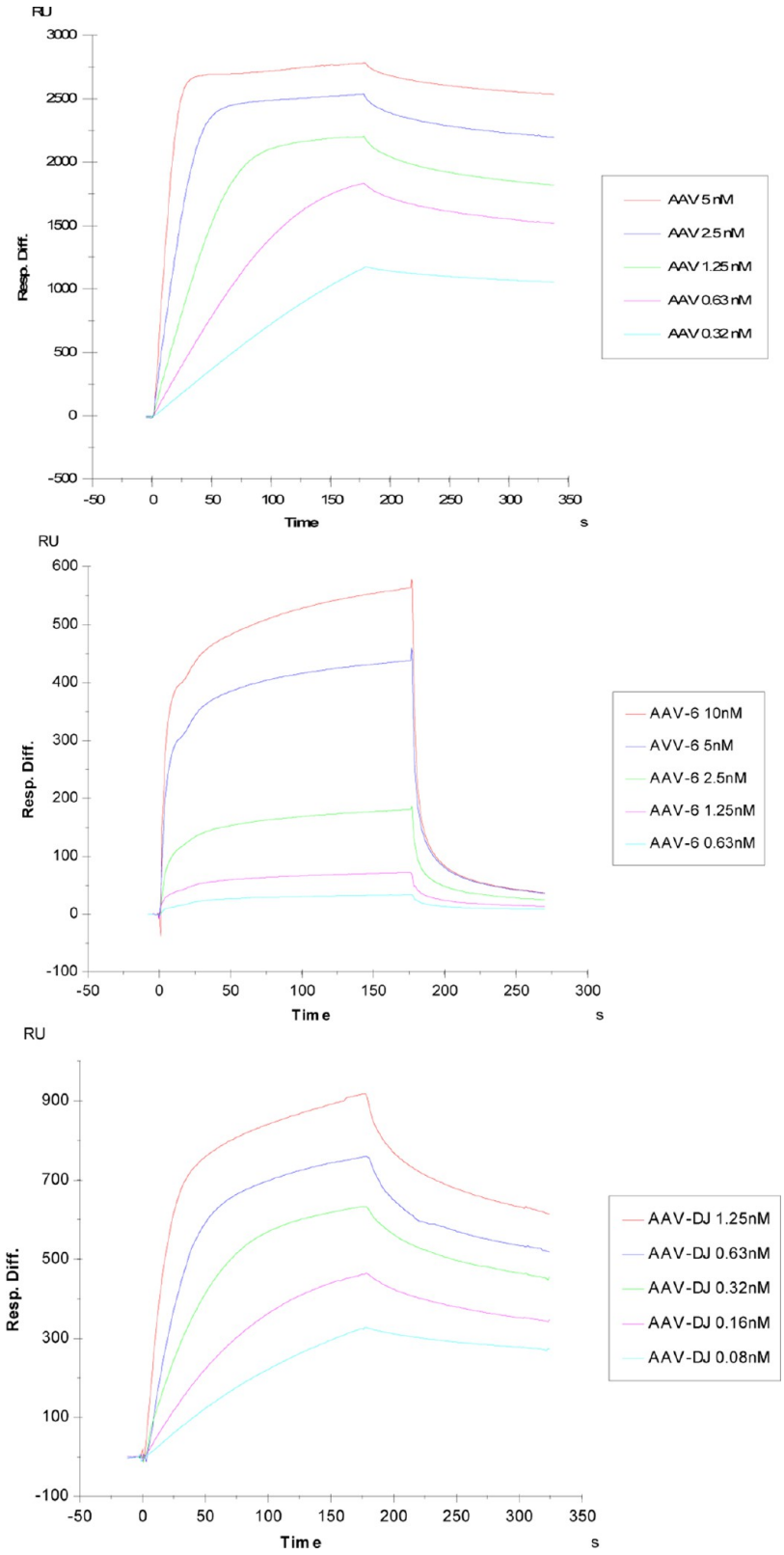

Figure 2. SPR sensorgrams of the AAV-2–heparin interaction (top). Concentrations of AAV were 5, 2.5, 1.25, 0.63, and 0.32 nM (from top to bottom, respectively). SPR sensorgrams of the AAV-6–heparin interaction (middle). Concentrations of AAV were 10, 5, 2.5, 1.25, and 0.63 nM (from top to bottom, respectively). SPR sensorgrams of the AAV-DJ–heparin interaction (bottom). Concentrations of AAV were 1.25, 0.63, 0.32, 0.16, and 0.08 nM (from top to bottom, respectively).

followed methods developed for AAV-2[48] that used the Bac-to-Bac Baculovirus Expression Vector System (Invitrogen) and were adapted for AAV-DJ as previously described.[49] VLPs are devoid of infectious viral DNA, but the outer protein capsids appear to be structurally and functionally identical to the wild-type virus. These empty capsids were purified by three rounds

dx.doi.org/10.1021/bi4008676 | *Biochemistry* 2013, 52, 6275–6285

of CsCl density gradient ultracentrifugation, followed by heparin affinity chromatography, eluting with a NaCl gradient. AAV-6 was prepared in HeLa cells as infectious virions and purified by three rounds of CsCl gradient ultracentrifugation, all using protocols that have been described previously.[50] All samples were dialyzed into phosphate-buffered saline [137 mM NaCl, 2.7 mM KCl, 10 mM Na_2HPO_4, and 1.8 mM KH_2PO_4 (pH 7.4)].

Preparation of the Heparin Biochip. The biotinylated heparin was prepared by reaction of sulfo-*N*-hydroxysuccinimide long chain biotin (Piece, Rockford, IL) with the free amino groups of unsubstituted glucosamine residues in the polysaccharide chain, following a published procedure.[51] The biotinylated heparin was immobilized to a streptavidin (SA) chip using the manufacturer's protocol. In brief, a 20 μL solution of the heparin−biotin conjugate (0.1 mg/mL) in HBS-EP running buffer was injected over flow cell 2 (FC2) of the SA chip, at a flow rate of 10 μL/min. The successful immobilization of heparin was confirmed by the observation of an ∼50 resonance unit (RU) increase in the sensor chip. The control flow cell (FC1) was prepared by a 1 min injection with saturated biotin.

Measurement of the Interaction between Heparin and AAV Using BIAcore SPR. The protein samples were diluted in HBS-EP buffer [0.01 M HEPES, 0.15 M NaCl, 3 mM EDTA, and 0.005% surfactant P20 (pH 7.4)]. Different dilutions of protein samples were injected at a flow rate of 30 μL/min. At the end of the sample injection, the same buffer was passed over the sensor surface to facilitate dissociation. After dissociation for of 3 min, the sensor surface was regenerated with 30 μL of 0.5% SDS and then with 2 M NaCl to yield a fully regenerated surface. The response was monitored as a function of time (sensorgram) at 25 °C.

Inhibition of Heparin Binding by Oligosaccharides. AAV-2 at 8.3 pM (equivalent to capsid protein at 0.5 nM) was mixed with 1000 nM heparin oligosaccharides, including disaccharide (dp2), tetrasaccharide (dp4), hexasaccharide (dp6), octasaccharide (dp8), decasaccharide (dp10), tetradecasaccharide (dp14), hexadecasaccharide (dp16), and octadecasaccharide (dp18), all in HBS-EP buffer. Samples were injected over the heparin chip at a flow rate of 30 μL/min. After each run, dissociation and regeneration were performed as described above. For each set of competition experiments on SPR, a control experiment (target without ligand) was performed to make sure the surface was completely regenerated and that the results obtained between runs were comparable.

Inhibition of Heparin Binding by GAGs and Chemically Modified Heparin. AAV-2 at 8.3 pM was premixed with 100 nM GAG or chemically modified heparin. Otherwise, SPR was performed as described above.

Atomic Force Microscopy. AAV-2 was combined with 100 nM GAG and incubated at 22 °C for 10 min. A 20 μL aliquot was spotted on a sheet of immobilized mica and allowed to set for 1 h before being washed with Milli-Q water. The sample was dried for 6 h. Raster images were obtained using 10 μm squares, and a representative area was rescanned at a higher resolution with 2 μm squares. Using Asylum Research version 6.22, particle heights were obtained for the 10 μm squares in representative sections.

RESULTS

Kinetics of the AAV−Heparin Interactions. The binding to immobilized heparin was measured for the three virions (AAV-2, AAV-6, and AAV-DJ) using SPR. The SPR binding sensorgrams of the AAV-2−heparin, AAV-6−heparin, and AAV-DJ−heparin interactions are displayed in Figure 2 showing different binding profiles. The sensorgrams were fit globally to obtain apparent on (k_a) and off (k_b) rates for the binding equilibrium (Table 1), using the BiaEvaluation software and assuming a 1:1 Langmuir model.

Table 1. Summary of the Kinetic Data of AAV−Heparin Interactions

interaction	k_a (M^{-1} s^{-1})	k_d (s^{-1})	K_D (M)
AAV-2−heparin	1.2×10^7	1.2×10^{-3}	1.0×10^{-10}
AAV-6−heparin	1.61×10^6	0.0197	1.22×10^{-8}
AAV-DJ−heparin	4.3×10^7	4.6×10^{-3}	1.1×10^{-10}

Polymer Length. Relative avidity, determined through SPR measurements of AAV-2−heparin binding inhibited by different oligosaccharides, was used to establish the dependence of binding on saccharide chain length. These heparin-derived oligosaccharides ranged from disaccharides to octadecasaccharides (dp2 to dp18). The extent of competitive inhibition increases in two steps, once near a chain length of four saccharide units, and the other at 16 saccharide units (Figure 3). This can be rationalized if the binding sites on the side of each spike are approximately five saccharides in length, and if a chain length of 16 saccharide units is the minimum for a polysaccharide to bind to two neighboring sites on spikes related by one of the viral 3-fold axes of symmetry.[52]

Specificity for Different GAGs. The SPR competition assay was also utilized to determine the preferences of AAV-2 in binding to various GAGs (Figure 1). SPR competition sensorgrams and inhibition levels are displayed in Figure 4. The results showed that CSE provided the strongest inhibitory effect (70−80%) in terms of binding of AAV-2 to immobilized heparin. DiS-DS also inhibited binding by ∼40%. Other GAGs and SOS (as a non-GAG polyanion control) had little effect. The data suggest that the binding interactions are dependent on GAG structure and strongly influenced by the level of GAG sulfation.

Chemically Modified Heparins. SPR competition sensorgrams and inhibition profiles with chemically modified heparins are displayed in Figure 5 for AAV-2. Inhibitory activity is lost upon all types of desulfation (fully desulfated heparin, N-desulfated heparin, 2-O-desulfated heparin, and 6-O-desulfated heparin). However, with 2-O-desulfated heparin, the extent of the loss of inhibition is much smaller with AAV-2. This implies that *N*-sulfo groups and 6-*O*-sulfo groups are more critical than 2-*O*-sulfo groups to the AAV-2−heparin binding interaction.

AFM Analysis. In the absence of heparin oligosaccharides, AFM shows a field of approximately round particles of AAV-2 with heights in the range of 15−30 nm (Figure 6). This is consistent with particle heights reported earlier by Chen and the observation that empty particles were measured with somewhat reduced diameters because of deformation under the ATM tip.[59,60] In the presence of heparin oligosaccharides, the average particle size increases with chain length, indicating aggregation (Table 2 and Figure 6). Even at dp6, some larger particles are observed, suggesting a limited ability to cross-link. There is a marked increase in both the average size and the frequency of larger aggregates in dp14, dp16, and full-length heparin. The large particles 60−90 nm in height seen with dp16 oligosaccharides and dominant with heparin correspond to

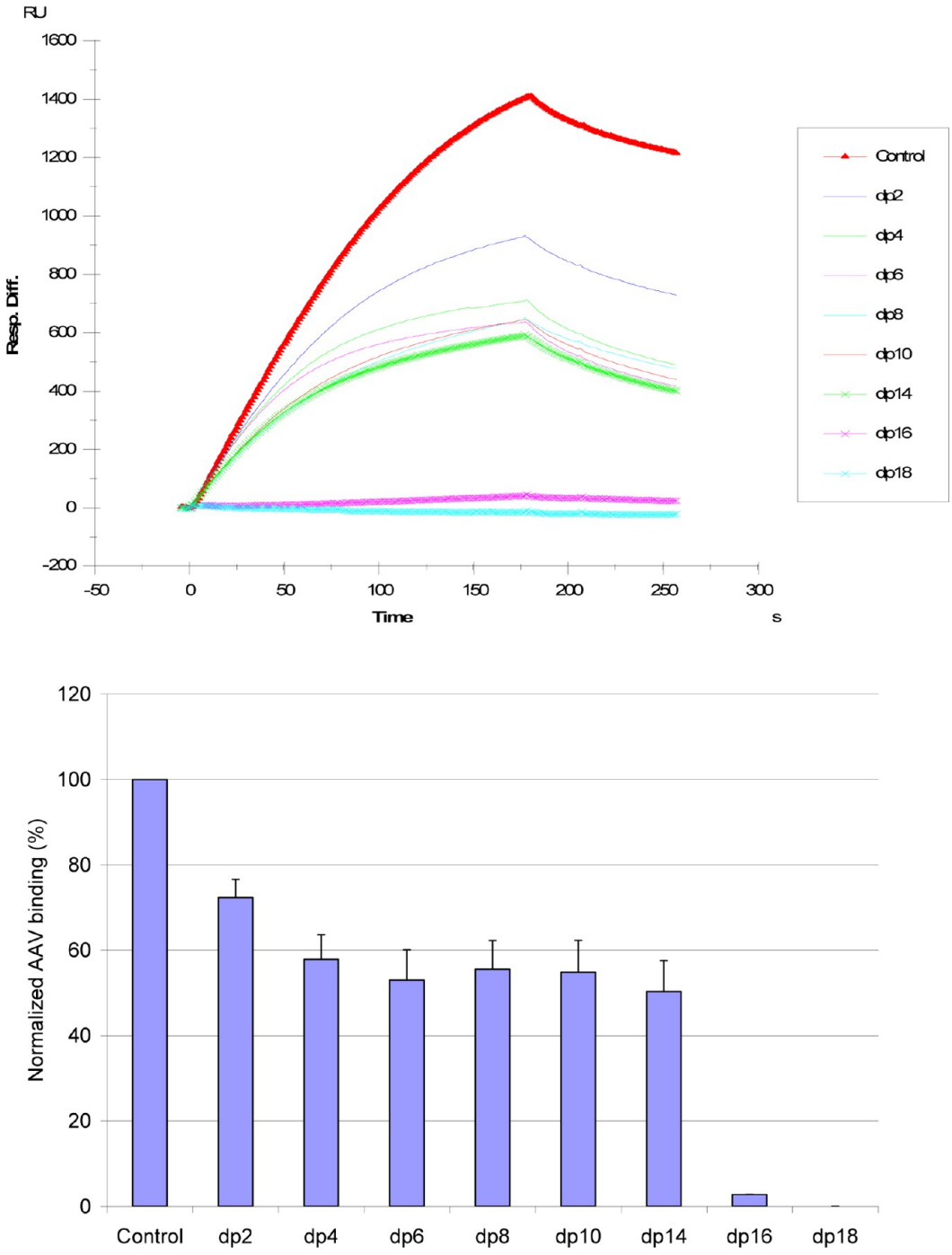

Figure 3. Sensorgrams for the AAV-2–heparin interaction inhibited by solution oligosaccharides of different chain length. The AAV-2 concentration was 0.5 nM, and concentrations of heparin oligosaccharides were 1000 nM. Bar graphs (errors from triplicate experiments) showing relative levels of AAV-2 binding in the presence of competing heparin oligosaccharides.

several particle diameters and indicate the improving ability of multiple virions to be bound along the GAG chain and of each particle to host interactions with multiple GAGs, presumably at binding sites related by icosahedral symmetry.

Molecular Modeling. An extended chain model of $[\beta$-D-GlcA-(1,4′)-α-D-GlcNAc-(1,4′)$]_8$ was generated using the GLYCAM Web tool (http://www.glycam.com).[53] This was fit into the difference density obtained by subtracting the cryo-electron microscopy (cryo-EM) reconstruction of AAV-2 from that of the AAV-2–heparin complex at 8.3 Å resolution.[52] Coot[54] was used for computer-aided manual fitting of the model into the difference density contoured at 6σ. Stereochemical distortions, introduced during modeling, were corrected through molecular mechanics energy minimization using NAMD.[55] Before final energy minimization with NAMD and checking of stereochemical parameters, close contacts with the virus were resolved and the fit to density was improved using Coot. Figure 7 was generated using PyMol.[56]

DISCUSSION

Through SPR, we now have fully quantitative measures of the avidity of AAV for heparin. Prior quantitation used the proxy of

dx.doi.org/10.1021/bi4008676 | *Biochemistry* 2013, 52, 6275–6285

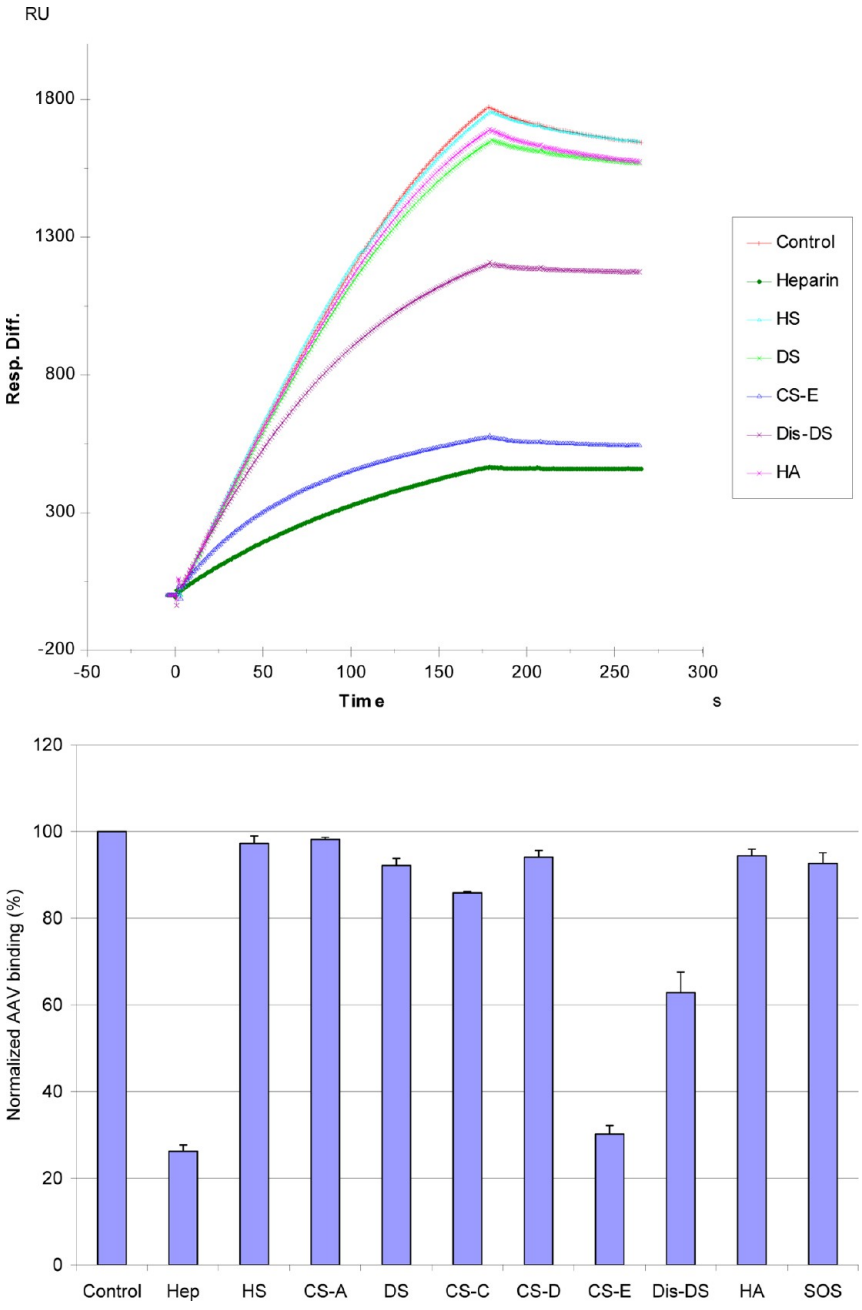

Figure 4. Sensorgrams for the AAV-2–heparin interaction inhibited by GAGs of various types. The AAV-2 concentration was 0.5 nM, and concentrations of GAGs were 100 nM. Bar graphs (errors from triplicate experiments) showing relative levels of AAV-2 binding in the presence of different competing GAGs.

NaCl concentration needed to elute AAV from a heparin affinity column for rank ordering.[29,35,36] Heparin affinity elution had shown that, of natural serotypes, AAV-2 binds strongest and AAV-6 weakest of those measurable. SPR is consistent with this and now shows a 100-fold difference in avidity (Table 1). AAV-DJ is a chimeric combination of AAV-2, -8, and -9 created by random gene shuffling, followed by selection for liver cell transduction and escape from human polyclonal neutralizing sera.[11] There are several potential causes for the improved *in vivo* (mouse) hepatotropism, of which altered attachment has been considered a possibility. SPR, like heparin affinity[49] and cell binding,[11] indicates weakened binding relative to that of AAV-2. Quantitatively, the SPR-derived 10% difference in the apparent K_D (Table 1) is consistent with the structures of AAV-2 and AAV-DJ being very similar in the heparin-binding region, and differing in calculated electrostatic potential only on the periphery of the binding site.[49,57] A 10% difference in binding avidity is unlikely to account, through cell attachment alone, for >10-fold differences in *in vitro* transduction efficiencies and *in vivo* tissue tropism.[11] Suspicion then naturally falls on the region of the structure where there are the greatest differences, the external loop that constitutes variable region 1. Given that this is the center of the AAV-2 epitope for neutralizing monoclonal antibody A20,[58] it is likely that structural differences resulted here from AAV-DJ's stringent selection by escape from neutralizing sera.[11] It is possible that changed tissue tropism *in vivo* results from altered immune clearance, sequestration, or other effects. As for changes to transduction *in*

dx.doi.org/10.1021/bi4008676 | *Biochemistry* 2013, 52, 6275–6285

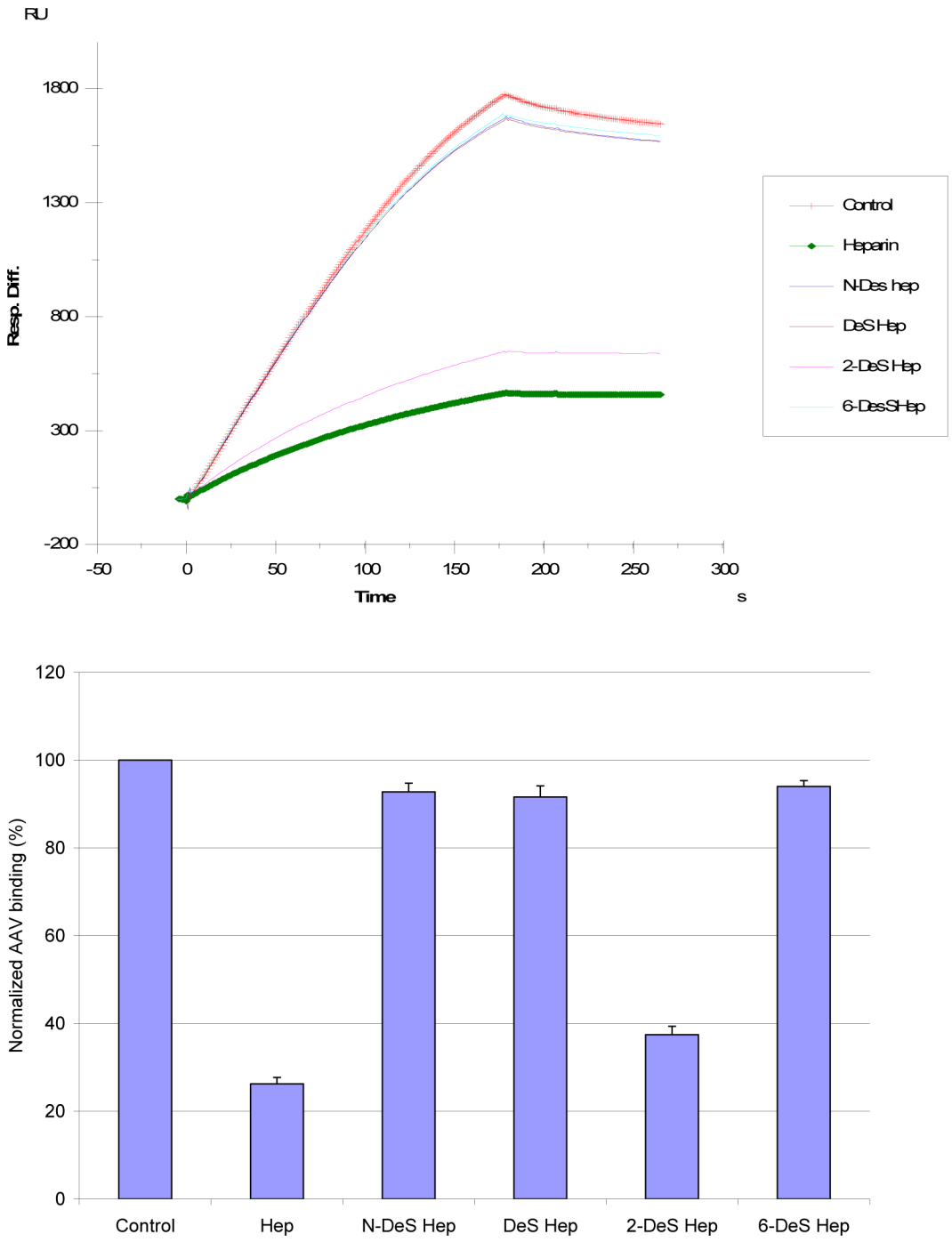

Figure 5. Sensorgrams for the AAV-2−heparin interaction inhibited by heparins that have been chemically desulfonated in various ways. The AAV-2 concentration was 0.5 nM, and concentrations of chemically modified heparin were 100 nM. Bar graphs (errors from triplicate experiments) showing relative levels of AAV-2 binding in the presence of GAGs with different sulfonation patterns.

vitro, quantitatively similar dissociation constants draw attention away from initial attachment to speculation that selection of neutralization escape variants may have serendipitously altered coreceptor binding, if neutralizing epitopes are well-represented at currently uncharacterized coreceptor binding sites.

The dependence of AAV-2−GAG interactions on chain length can be interpreted in light of the cryo-EM structure of AAV-2 complexed with a 17 kDa fragment of heparin (Figure 7).[52] The heparin in the cryo-EM visualization lacks molecular detail, because of the modest 8 Å experimental resolution, and because we see the average of heterogeneous sequences that are bound to the thousands of particles imaged. The virus structure in the complex is better defined, because the 3 Å resolution crystal structure[57] can be docked as a rigid body by superimposing the icosahedral symmetry. The maximal heparin density, implying the tightest binding, is adjacent to Arg_{585} and Arg_{588}. Strong density extends about the length of a pentasaccharide to cover other positively charged residues implicated by mutagenesis in heparin binding: Arg_{484}, Arg_{487}, and Lys_{532},[31,59] as well as Lys_{527}. With short oligosaccharides, Figure 5B shows progressively stronger binding, until

dx.doi.org/10.1021/bi4008676 | *Biochemistry* 2013, 52, 6275−6285

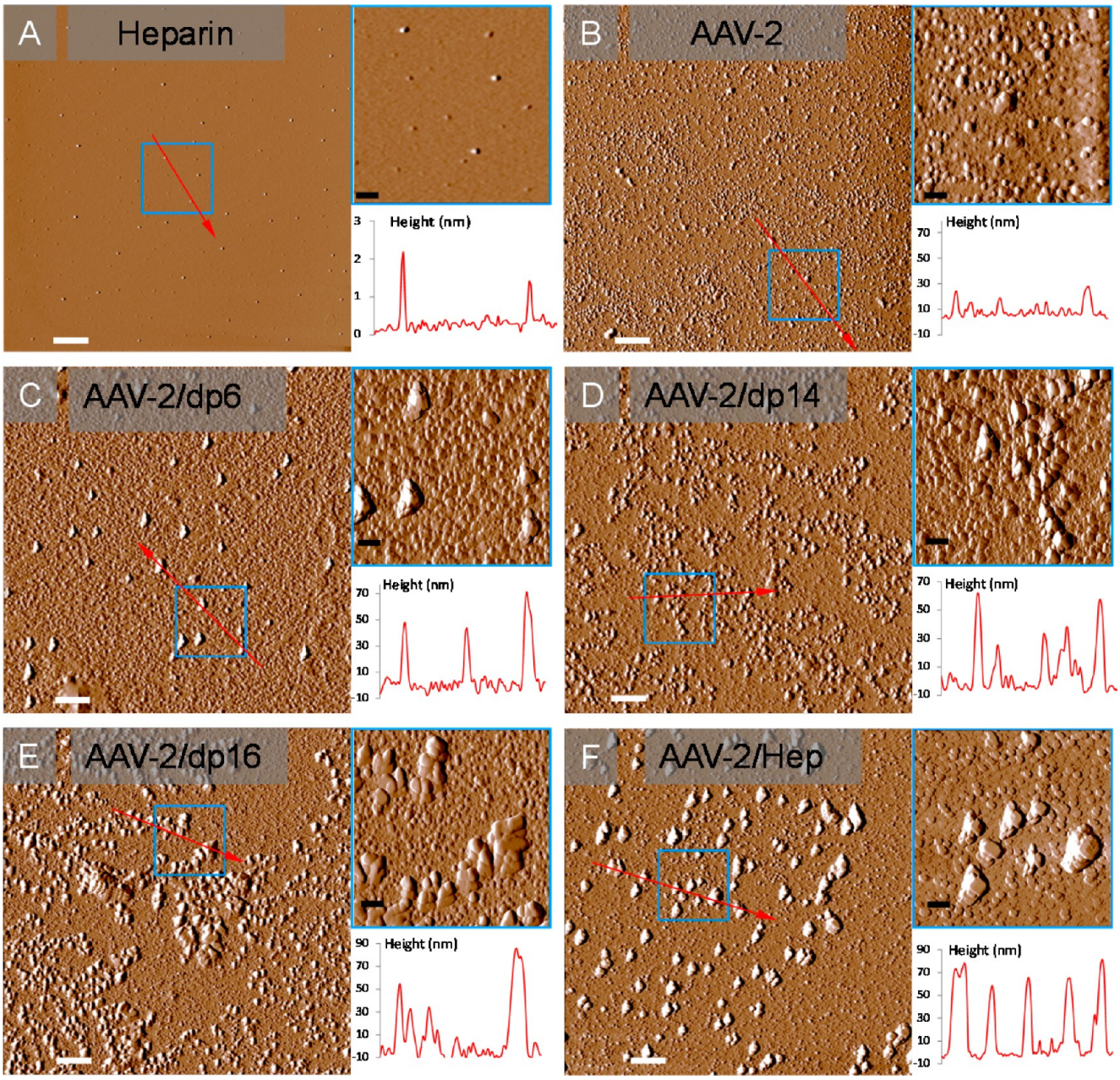

Figure 6. AFM images of AAV-2 and complexes with different heparin oligosaccharides. (A) Heparin alone (control). (B) AAV-2 particles alone (control). (C) AAV-2–heparin dp6 complexes. (D) AAV-2–heparin dp14 complexes. (E) AAV-2–heparin dp16 complexes. (F) AAV-2–heparin (full chain) complexes. White and black scale bars represent 1 and 250 nm, respectively. All panels show 10 μm images. The top insets are expansions (5 times) of the areas depicted in small blue squares, and the bottom insets are particle height distributions along the red arrows.

Table 2. Description of Particle Heights Observed via AFM on AAV-2–Heparin Oligosaccharide Complexes

	predominant particle size range	minor particle morphologies
AAV-2 only	15–30 nm	
AAV-2–dp6	15–30 nm	30–80 nm
AAV-2–dp14	15–30 nm	30–80 nm
AAV-2–dp16	15–60 nm	60–90 nm
AAV-2–heparin	60–90 nm	15–30 nm

presumably all the main interactions of a single site on AAV are contributing. The next big change comes between dp14 and dp16, which might correspond to the chain length required for a change in avidity with the contribution of two symmetry-related sites on the virus. Density bridging between adjacent sites in the EM reconstruction is approximately half the maximal height, implying looser association, but still experimentally significant at 6σ. Modeling a canonical glycosaminoglycan through the path of this density shows that a minimal chain length of 13 is required to make contacts with two symmetry-related copies of Lys_{532} (Figure 7). Intriguingly, density continues away from the 3-fold axis in each direction such that a 16-mer can be fit into the EM density. This indicates continuing GAG–virus interactions beyond Lys_{532}. It may be that the stronger binding of dp16 evident in Figure 5B and the length of the density seen in the EM reconstruction are both consequences of two-site attachment becoming optimal with a chain length of at least 15. Some caution is warranted,

dx.doi.org/10.1021/bi4008676 | *Biochemistry* 2013, 52, 6275–6285

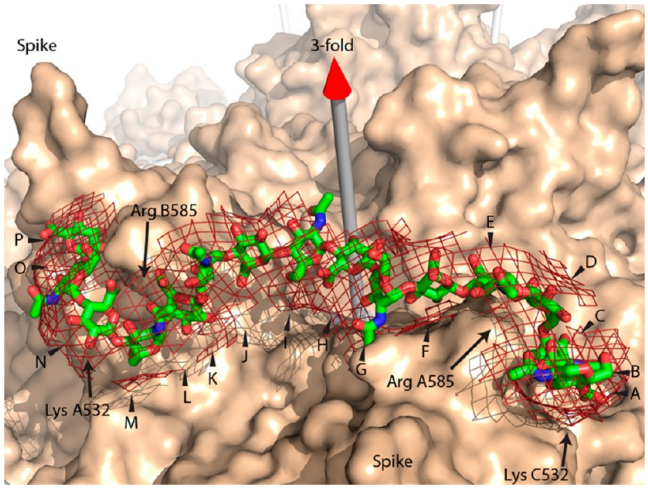

Figure 7. Binding of oligosaccharides to AAV-2. A 16-residue glycosaminoglycan (GAG) stick model has been fit approximately into the heparin difference density from a cryo-EM study at 8 Å resolution[52] that is shown as a net at a 6σ contour level on top of the van der Waals surface of the AAV-2 crystal structure.[57] The GAG oligomer is modeled bridging between 3-fold symmetry-related binding sites on the sides of adjacent viral spikes. A chain length of at least 13 is needed to make contact with the five positively charged residues implicated at each of two binding sites. Density extending over 16 residues (lettered A–P) suggests additional interactions and the possibility that the stronger binding of a 16-mer in Figure 5 might correspond to an increase in avidity with optimization of two-site binding. Note that a single asymmetric oligosaccharide chain passing through two symmetry-related binding sites must have somewhat different interactions, suggesting that the binding sites have evolved some adaptability.

because structures much better than 8 Å resolution would be needed to estimate the strength of atomic interactions at the ends of the 16-mer. Nonetheless, with indications from both the EM and the current binding studies, the body of evidence that AAV might get wrapped by GAGs binding at two or more sites is growing, with an interesting implication. If at one site the polysaccharide is bound running toward the 3-fold axis, at the adjacent binding site it is running away. Thus, a single polysaccharide chain cannot match the viral symmetry at adjacent sites, and therefore, the site must be tolerant of binding in either direction.

The inhibitory effects of soluble GAGs on the AAV–immobilized heparin interaction were greatest for heparin with 2.8 mol of sulfo groups per disaccharide repeating unit, followed by CS-E and Dis-DS with 1.5–2 mol of sulfo groups per disaccharide and then HS, DS, CS-A, and CS-C with $\leq$1 mol of sulfo groups per disaccharide. Combining the structural requirements in the modified heparin and chondroitin/dermatan family of the GAGs suggests an AAV binding motif that prefers disaccharide units with two sulfo groups on a hexosamine residue linked to a uronic acid having a carboxyl group. On heparin, these two charged groups per disaccharide repeating unit are *N*-sulfo and 6-*O*-sulfo groups and on the chondroitin/dermatan family are the 4-*O*-sulfo and 6-*O*-sulfo groups found on CS-E or Dis-DS. These results are similar to the GAG sulfation preferences of other proteins, such as Shh, Ihog, FGF1, FGF2, and CrataBL.[60−62]

Prior to this work, nothing was known about the internal sequence preferences within the GAGs to which AAVs attach. While much remains to be elucidated for a full characterization of any of the serotypes, the inhibition patterns for heparins desulfated at specific locations begin to offer guiding principles. The presence of sulfo groups at the N- and 6-O-positions is more critical than at the 2-O-position. Such information might support the first step in an interactive process through which one might hone in on heparin oligomers with stronger binding and inhibitory activity, and thereby advance our understanding of AAV attachment by combining structural and virological studies.

AUTHOR INFORMATION

Corresponding Authors

*Department of Biochemistry and Molecular Biology, School of Medicine, Oregon Health & Science University, Portland, OR 97239. Telephone: (503) 494-1025. Fax: (503) 494-8393. E-mail: chapmami@ohsu.edu.

*Department of Chemistry and Chemical Biology, Center for Biotechnology and Interdisciplinary Studies, Rensselaer Polytechnic Institute, Troy, NY 12180. Telephone: (518) 276-3404. Fax: (518) 276-3405. E-mail: linhar@rpi.edu.

Funding

This work was supported by grants from the National Institutes of Health (GM-38060 to R.J.L. and GM66875 to M.S.C.) and a Pilot Project Grant from the Oregon Health & Science University Center for Spatial Systems Biomedicine to M.S.C. T.F.L. was supported by an Interactions at Microbe-Host Interface training grant from the National Institutes of Health (T32AI007472).

Notes

The authors declare no competing financial interest.

ABBREVIATIONS

GAG, glycosaminoglycan; AAV, adeno-associated virus; SPR, surface plasmon resonance; AFM, atomic force microscopy; LMWH, low-molecular weight heparin; HS, heparan sulfate; PG, proteoglycan; CS-A, chondroitin sulfate A; DS, dermatan sulfate; Dis-DS, dermatan disulfate; CS-C, chondroitin sulfate C; CS-D, chondroitin sulfate D; CS-E, chondroitin sulfate E; SOS, sucrose octasulfate; SA, streptavidin; dp, degree of polymerization; HA, hyaluronan.

REFERENCES

(1) Muzyczka, N., and Berns, K. I. (2001) *Parvoviridae*: The Viruses and Their Replication. In *Virology* (Fields, B. N., Knipe, D. M., and Howley, P. M., Eds.) 4th ed., pp 2327–2360, Lippincott Williams & Wilkins, Philadelphia.

(2) Schambach, A., Maetzig, T., and Baum, C. (2008) Retroviral vectors for Cell and Gene Therapy. In *Gene and cell therapy: Therapeutic mechanisms and strategies* (Templeton, N. S., Ed.) pp 3–15, CRC Press, Boca Raton, FL.

(3) Simonelli, F., Maguire, A. M., Testa, F., Pierce, E. A., Mingozzi, F., Bennicelli, J. L., Rossi, S., Marshall, K., Banfi, S., Surace, E. M., Sun, J., Redmond, T. M., Zhu, X., Shindler, K. S., Ying, G. S., Ziviello, C., Acerra, C., Wright, J. F., McDonnell, J. W., High, K. A., Bennett, J., and Auricchio, A. (2010) Gene therapy for Leber's congenital amaurosis is safe and effective through 1.5 years after vector administration. *Mol. Ther. 18*, 643–650.

(4) Cideciyan, A. V., Hauswirth, W. W., Aleman, T. S., Kaushal, S., Schwartz, S. B., Boye, S. L., Windsor, E. A. M., Conlon, T. J., Sumaroka, A., Roman, A. J., Byrne, B. J., and Jacobson, S. G. (2009) Vision 1 Year after Gene Therapy for Leber's Congenital Amaurosis. *N. Engl. J. Med. 361*, 725–727.

(5) Nathwani, A. C., Tuddenham, E. G., Rangarajan, S., Rosales, C., McIntosh, J., Linch, D. C., Chowdary, P., Riddell, A., Pie, A. J.,

Harrington, C., O'Beirne, J., Smith, K., Pasi, J., Glader, B., Rustagi, P., Ng, C. Y., Kay, M. A., Zhou, J., Spence, Y., Morton, C. L., Allay, J., Coleman, J., Sleep, S., Cunningham, J. M., Srivastava, D., Basner-Tschakarjan, E., Mingozzi, F., High, K. A., Gray, J. T., Reiss, U. M., Nienhuis, A. W., and Davidoff, A. M. (2011) Adenovirus-associated virus vector-mediated gene transfer in hemophilia B. *N. Engl. J. Med. 365*, 2357−2365.

(6) Samulski, R. J., Zhu, X., Xiao, X., Brook, J. D., Housman, D. E., Epstein, N., and Hunter, L. A. (1991) Targeted Integration of Adenoassociated virus (AAV) into Human Cheomosome-19. *EMBO J. 10*, 3941−3950.

(7) Dyall, J., Szabo, P., and Berns, K. I. (1999) Adeno-associated virus (AAV) site-specific integration: Formation of AAV-AAVS1 junctions in an in vitro system. *Proc. Natl. Acad. Sci. U.S.A. 96*, 12849−12854.

(8) Huttner, N. A., Girod, A., Schnittger, S., Schoch, C., Hallek, M., and Buning, H. (2003) Analysis of site-specific transgene integration following cotransduction with recombinant adeno-associated virus and a rep encodingplasmid. *J. Gene Med. 5*, 120−129.

(9) Carter, B. J., Burstein, H., and Peluso, R. W. (2008) Adeno-associated Virus and AAV Vectors for Gene delivery. In *Gene and cell therapy: Therapeutic mechanisms and strategies* (Templeton, N. S., Ed.) pp 115−156, CRC Press, Boca Raton, FL.

(10) Gao, G., Lu, Y., Calcedo, R., Grant, R. L., Bell, P., Wang, L., Figueredo, J., Lock, M., and Wilson, J. M. (2006) Biology of AAV serotype vectors in liver-directed gene transfer to nonhuman primates. *Mol. Ther. 13*, 77−87.

(11) Grimm, D., Lee, J. S., Wang, L., Desai, T., Akache, B., Storm, T. A., and Kay, M. A. (2008) In vitro and in vivo gene therapy vector evolution via multispecies interbreeding and retargeting of adeno-associated viruses. *J. Virol. 82*, 5887−5911.

(12) Kotchey, N. M., Adachi, K., Zahid, M., Inagaki, K., Charan, R., Parker, R. S., and Nakai, H. (2011) A potential role of distinctively delayed blood clearance of recombinant adeno-associated virus serotype 9 in robust cardiac transduction. *Mol. Ther. 19*, 1079−1089.

(13) Halbert, C. L., Standaert, T. A., Wilson, C. B., and Miller, A. D. (1998) Successful readministration of adeno-associated virus vectors to the mouse lung requires transient immunosuppression during the initial exposure. *J. Virol. 72*, 9795−9805.

(14) Asokan, A., Hamra, J. B., Govindasamy, L., Agbandje-McKenna, M., and Samulski, R. J. (2006) Adeno-associated virus type 2 contains an integrin $\alpha5\beta1$ binding domain essential for viral cell entry. *J. Virol. 80*, 8961−8969.

(15) Kashiwakura, Y., Tamayose, K., Iwabuchi, K., Hirai, Y., Shimada, T., Matsumoto, K., Nakamura, T., Watanabe, M., Oshimi, K., and Daida, H. (2005) Hepatocyte growth factor receptor is a coreceptor for adeno-associated virus type 2 infection. *J. Virol. 79*, 609−614.

(16) Ling, C., Lu, Y., Kalsi, J. K., Jayandharan, G. R., Li, B., Ma, W., Cheng, B., Gee, S. W., McGoogan, K. E., Govindasamy, L., Zhong, L., Agbandje-McKenna, M., and Srivastava, A. (2010) Human hepatocyte growth factor receptor is a cellular coreceptor for adeno-associated virus serotype 3. *Hum. Gene Ther. 21*, 1741−1747.

(17) Pasquale, G. D., Davidson, B. L., Stein, C. S., Martins, I., Scudiero, D., Monks, A., and Chiorini, J. A. (2003) Identification of PDGFR as a receptor for AAV-5 transduction. *Nat. Med. 9*, 1306−1312.

(18) Qing, K., Mah, C., Hansen, J., Zhou, S., Dwarki, V., and Srivastava, A. (1999) Human fibroblast growth factor receptor 1 is a co-receptor for infection by adeno-associated virus 2. *Nat. Med. 5*, 71−77.

(19) Akache, B., Grimm, D., Pandey, K., Yant, S. R., Xu, H., and Kay, M. A. (2006) The 37/67-kilodalton laminin receptor is a receptor for adeno-associated virus serotypes 8, 2, 3, and 9. *J. Virol. 80*, 9831−9836.

(20) Weller, M. L., Amornphimoltham, P., Schmidt, M., Gutkind, S., and Chiorini, J. A. (2009) Epidermal Growth Factor Receptor is a Receptor for Adeno-Associated Virus Serotype 6. In *American Society for Virology*, p 80, FASEB, Vancouver, BC.

(21) Varki, A., Cummings, R. D., Esko, J. D., Freeze, H. H., Stanley, P., Bertozzi, C. R., Hart, G. W., and Etzler, M. E., Eds. (2009) *Essentials of glycobiology*, 2nd ed., Cold Spring Harbor Laboratory Press, Plainview, NY.

(22) Patel, M., Yanagishita, M., Roderiquez, G., Bou-Habib, D. C., Oravecz, T., Hascall, V. C., and Norcross, M. A. (1993) Cell-surface heparan sulfate proteoglycan mediates HIV-1 infection of T-cell lines. *AIDS Res. Hum. Retroviruses 9*, 167−174.

(23) Saphire, A. C., Bobardt, M. D., and Gallay, P. A. (1999) Host cyclophilin A mediates HIV-1 attachment to target cells via heparans. *EMBO J. 18*, 6771−6785.

(24) Jackson, T., Ellard, F. M., Ghazaleh, R. A., Brookes, S. M., Blakemore, W. E., Corteyn, A. H., Stuart, D. I., Newman, J. W., and King, A. M. (1996) Efficient infection of cells in culture by type O foot-and-mouth disease virus requires binding to cell surface heparan sulfate. *J. Virol. 70*, 5282−5287.

(25) Zhang, W., Heil, M., Kuhn, R. J., and Baker, T. S. (2005) Heparin binding sites on Ross River virus revealed by electron cryo-microscopy. *Virology 332*, 511−518.

(26) Gillet, L., Colaco, S., and Stevenson, P. G. (2008) The Murid Herpesvirus-4 gL regulates an entry-associated conformation change in gH. *PLoS One 3*, e2811.

(27) Work, L. M., Buning, H., Hunt, E., Nicklin, S. A., Denby, L., Britton, N., Leike, K., Odenthal, M., Drebber, U., Hallek, M., and Baker, A. H. (2006) Vascular bed-targeted in vivo gene delivery using tropism-modified adeno-associated viruses. *Mol. Ther. 13*, 683−693.

(28) Perabo, L., Goldnau, D., White, K., Endell, J., Boucas, J., Humme, S., Work, L. M., Janicki, H., Hallek, M., Baker, A. H., and Buning, H. (2006) Heparan sulfate proteoglycan binding properties of adeno-associated virus retargeting mutants and consequences for their in vivo tropism. *J. Virol. 80*, 7265−7269.

(29) Wu, Z., Asokan, A., Grieger, J. C., Govindasamy, L., Agbandje-McKenna, M., and Samulski, R. J. (2006) Single Amino Acid Changes Can Influence Titer, Heparin Binding, and Tissue Tropism in Different Adeno-Associated Virus (AAV) Serotypes. *J. Virol. 80*, 11393−11397.

(30) Asokan, A., Conway, J. C., Phillips, J. L., Li, C., Hegge, J., Sinnott, R., Yadav, S., DiPrimio, N., Nam, H. J., Agbandje-McKenna, M., McPhee, S., Wolff, J., and Samulski, R. J. (2010) Reengineering a receptor footprint of adeno-associated virus enables selective and systemic gene transfer to muscle. *Nat. Biotechnol. 28*, 79−82.

(31) Kern, A., Schmidt, K., Leder, C., Muller, O. J., Wobus, C. E., Bettinger, K., Von der Lieth, C. W., King, J. A., and Kleinschmidt, J. A. (2003) Identification of a heparin-binding motif on adeno-associated virus type 2 capsids. *J. Virol. 77*, 11072−11081.

(32) Muller, O. J., Leuchs, B., Pleger, S. T., Grimm, D., Franz, W. M., Katus, H. A., and Kleinschmidt, J. A. (2006) Improved cardiac gene transfer by transcriptional and transductional targeting of adeno-associated viral vectors. *Cardiovasc. Res. 70*, 70−78.

(33) Handa, A., Muramatsu, S., Qiu, J., Mizukami, H., and Brown, K. E. (2000) Adeno-associated virus (AAV)-3-based vectors transduce haematopoietic cells not susceptible to transduction with AAV-2-based vectors. *J. Gen. Virol. 81*, 2077−2084.

(34) Summerford, C., and Samulski, R. J. (1998) Membrane-associated heparan sulfate proteoglycan is a receptor for adeno-associated virus type 2 virions. *J. Virol. 72*, 1438−1445.

(35) Lerch, T. F., and Chapman, M. S. (2012) Identification of the heparin binding site on adeno-associated virus serotype 3B (AAV-3B). *Virology 423*, 6−13.

(36) Xie, Q., Lerch, T. F., Meyer, N. L., and Chapman, M. S. (2011) Structure-function analysis of receptor-binding in adeno-associated virus serotype 6 (AAV-6). *Virology 420*, 10−19.

(37) Wu, Z., Miller, E., Agbandje-McKenna, M., and Samulski, R. J. (2006) $\alpha2,3$ and $\alpha2,6$ N-linked sialic acids facilitate efficient binding and transduction by adeno-associated virus types 1 and 6. *J. Virol. 80*, 9093−9103.

(38) Kaludov, N., Brown, K. E., Walters, R. W., Zabner, J., and Chiorini, J. A. (2001) Adeno-associated virus serotype 4 (AAV4) and AAV5 both require sialic acid binding for hemagglutination and efficient transduction but differ in sialic acid linkage specificity. *J. Virol. 75*, 6884−6893.

(39) Shen, S., Bryant, K. D., Sun, J., Brown, S. M., Troupes, A., Pulicherla, N., and Asokan, A. (2012) Glycan binding avidity determines the systemic fate of adeno-associated virus type 9. *J. Virol. 86*, 10408−10417.
(40) Bell, C. L., Gurda, B. L., Van Vliet, K., Agbandje-McKenna, M., and Wilson, J. M. (2012) Identification of the galactose binding domain of the AAV9 capsid. *J. Virol. 86*, 7326−7333.
(41) Capila, I., and Linhardt, R. J. (2002) Heparin-protein interactions. *Angew. Chem., Int. Ed. 41*, 391−412.
(42) Hacker, U., Nybakken, K., and Perrimon, N. (2005) Heparan sulphate proteoglycans: The sweet side of development. *Nat. Rev. Mol. Cell Biol. 6*, 530−541.
(43) Parish, C. R. (2006) The role of heparan sulphate in inflammation. *Nat. Rev. Immunol. 6*, 633−643.
(44) Powell, A. K., Yates, E. A., Fernig, D. G., and Turnbull, J. E. (2004) Interactions of heparin/heparan sulfate with proteins: Appraisal of structural factors and experimental approaches. *Glycobiology 14*, 17R−30R.
(45) Sasisekharan, R., Raman, R., and Prabhakar, V. (2006) Glycomics approach to structure-function relationships of glycosaminoglycans. *Annu. Rev. Biomed. Eng. 8*, 181−231.
(46) Brister, S. J., Buchanan, M. R., Griffin, C. C., Van Gorp, C. L., and Linhardt, R. J. (1999) Dermatan disulfate, an inhibitor of thrombin and complement activation. U.S. Patent 5,922,690.
(47) Yates, E. A., Santini, F., Guerrini, M., Naggi, A., Torri, G., and Casu, B. (1996) ^{1}H and ^{13}C NMR spectral assignments of the major sequences of twelve systematically modified heparin derivatives. *Carbohydr. Res. 294*, 15−27.
(48) Urabe, M., Ding, C., and Kotin, R. M. (2002) Insect cells as a factory to produce adeno-associated virus type 2 vectors. *Hum. Gene Ther. 13*, 1935−1943.
(49) Lerch, T. F., O'Donnell, J. K., Meyer, N. L., Xie, Q., Taylor, K. A., Stagg, S. M., and Chapman, M. S. (2012) Structure of AAV-DJ, a Retargeted Gene Therapy Vector: Cryo-Electron Microscopy at 4.5 Å Resolution. *Structure 20*, 1310−1320.
(50) Xie, Q., Ongley, H. M., Hare, J., and Chapman, M. S. (2008) Crystallization and preliminary X-ray structural studies of adeno-associated virus serotype 6. *Acta Crystallogr. F64*, 1074−1078.
(51) Hernaiz, M., Liu, J., Rosenberg, R. D., and Linhardt, R. J. (2000) Enzymatic modification of heparan sulfate on a biochip promotes its interaction with antithrombin III. *Biochem. Biophys. Res. Commun. 276*, 292−297.
(52) O'Donnell, J., Taylor, K. A., and Chapman, M. S. (2009) Adeno-associated virus-2 and its primary cellular receptor: Cryo-EM structure of a heparin complex. *Virology 385*, 434−443.
(53) Kirschner, K. N., Yongye, A. B., Tschampel, S. M., Gonzalez-Outeirino, J., Daniels, C. R., Foley, B. L., and Woods, R. J. (2008) GLYCAM06: A generalizable biomolecular force field. Carbohydrates. *J. Comput. Chem. 29*, 622−655.
(54) Emsley, P., Lohkamp, B., Scott, W. G., and Cowtan, K. (2010) Features and development of Coot. *Acta Crystallogr. D66*, 486−501.
(55) Phillips, J. C., Braun, R., Wang, W., Gumbart, J., Tajkhorshid, E., Villa, E., Chipot, C., Skeel, R. D., Kale, L., and Schulten, K. (2005) Scalable molecular dynamics with NAMD. *J. Comput. Chem. 26*, 1781−1802.
(56) DeLano, W. L. (2002) *The PyMOL Molecular Graphics System*, DeLano Scientific, San Carlos, CA.
(57) Xie, Q., Bu, W., Bhatia, S., Hare, J., Somasundaram, T., Azzi, A., and Chapman, M. S. (2002) The atomic structure of adeno-associated virus (AAV-2), a vector for human gene therapy. *Proc. Natl. Acad. Sci. U.S.A. 99*, 10405−10410.
(58) McCraw, D. M., O'Donnell, J. K., Taylor, K. A., Stagg, S. M., and Chapman, M. S. (2012) Structure of adeno-associated virus-2 in complex with neutralizing monoclonal antibody A20. *Virology 431*, 40−49.
(59) Opie, S. R., Warrington, K. H., Jr., Agbandje-McKenna, M., Jr., Zolotukhin, S., and Muzyczka, N. (2003) Identification of amino acid residues in the capsid proteins of adeno-associated virus type 2 that contribute to heparan sulfate proteoglycan binding. *J. Virol. 77*, 6995−7006.
(60) Zhang, F., McLellan, J. S., Ayala, A. M., Leahy, D. J., and Linhardt, R. J. (2007) Kinetic and structural studies on interactions between heparin or heparan sulfate and proteins of the hedgehog signaling pathway. *Biochemistry 46*, 3933−3941.
(61) Zhang, F., Zhang, Z., Lin, X., Beenken, A., Eliseenkova, A. V., Mohammadi, M., and Linhardt, R. J. (2009) Compositional analysis of heparin/heparan sulfate interacting with fibroblast growth factor·fibroblast growth factor receptor complexes. *Biochemistry 48*, 8379−8386.
(62) Zhang, F., Walcott, B., Zhou, D., Gustchina, A., Lasanajak, Y., Smith, D. F., Ferreira, R. S., Correia, M. T., Paiva, P. M., Bovin, N. V., Wlodawer, A., Oliva, M. L., and Linhardt, R. J. (2013) Structural Studies of the Interaction of *Crataeva tapia* Bark Protein with Heparin and Other Glycosaminoglycans. *Biochemistry 52*, 2148−2156.